Available on: http://gjetr.ep-journals.org/ E-ISSN: 3051-3782, P-ISSN: 3051-3774

Global Journal of Engineering and Technology Review

Volume: 02 Issue: 11 November 2026

Experimental Evaluation of a Photovoltaic Powered DC Heating System with Closed-Loop Temperature Control for a Hybrid Dryer

DARE, Aderonke Adekemi
Department of Electrical and Electronic Engineering, Faculty of Engineering and Technology, Lead City University, Ibadan, Oyo State, Nigeria
Orcid: 0009-00007459-7362

BABATUNDE, Steven Emmanuel
Department of Electrical and Electronic Engineering, Faculty of Engineering and Technology, Achievers University, Owo, Ondo state, Nigeria

ENOCHOGHENE, Samuel Oghenenyerovwo
Department of Electrical and Electronic Engineering, Faculty of Engineering and Technology, Lead City University, Ibadan, Oyo State, Nigeria

ADESINA, Olusegun Bola
Department of Electrical and Electronic Engineering, Faculty of Engineering and Technology, Lead City University, Ibadan, Oyo State, Nigeria

Published Date: November 11, 2026 **Article DOI : 10.65150/EP-gjetr/V2E11/2026-05**

ABSTRACT: Photovoltaic (PV)-powered electrical heating can provide a fast and controllable auxiliary heat source for hybrid agricultural dryers, but its effectiveness depends on stable DC power conversion and accurate thermal feedback. This study experimentally evaluates a PV-powered direct-current heating subsystem integrated into a modular hybrid dryer. The electrical subsystem used two 350 W PV modules in parallel, an adjustable 800 W DC–DC converter, and a 600 W, 35 V resistive heater. Chamber temperature was regulated by thermistor feedback through an SG3524 PWM controller, C1815 driver transistor and IRFP4468 MOSFET switching stage. The high-power heater was supplied directly from the PV array through the regulated converter, while the auxiliary battery served the low-power fan and control circuits. Measurements were recorded at 15-min intervals during a five-hour electrical control test and an eight-hour plantain drying experiment. Converter input voltage varied from 28.50 to 33.71 V while output voltage remained within 34.70– 35.00 V. Mean converter efficiency was 91.30% with a standard deviation of 0.29% and coefficient of variation of 0.32%. Mean steady-state heater power was 600.13 W, with a standard deviation of 1.97 W and coefficient of variation of 0.33%. Chamber temperature increased from 30.4 to 59.7 °C within approximately one hour and subsequently remained near the 60 °C set-point, giving a steady-state mean of 60.13 °C, standard deviation of 0.11 °C, coefficient of variation of 0.18%, mean absolute temperature error of 0.13 °C and maximum absolute deviation of 0.30 °C. In the associated drying test, 10 kg of fresh plantain at 65% wet-basis moisture content was reduced to approximately 10% in 8 h, with the maximum interval drying rate of 1.29 kg h^{-1} occurring at 1.75 h. The results demonstrate that direct PV-to-DC heating, when coupled with regulated power conversion and closed-loop electronic control, can provide a stable and responsive auxiliary heat source for modular hybrid drying.

KEYWORDS: Photovoltaic Heating, Temperature Regulation, Hybrid Dryer, DC heater, DC– DC Converter, Closed-loop Control.

1. INTRODUCTION

Drying is a critical postharvest operation because controlled moisture removal improves storage stability, reduces microbial deterioration and extends the usable life of agricultural produce. In many developing agricultural communities, however, drying remains dependent on open-air exposure or simple solar dryers whose thermal performance changes with solar radiation, ambient temperature and airflow. The attractiveness of solar drying is therefore accompanied by a basic engineering challenge: the available thermal input is renewable but intermittent. Hybrid dryers address this limitation by combining complementary heat sources, yet the addition of an auxiliary source does not by itself guarantee stable process temperature.

Recent research has moved toward hybrid systems that combine solar energy with biomass, electrical heating, energy storage and automated control. Hybrid solar-biomass systems have demonstrated the ability to extend operating periods and reduce dependence on a single energy source, while smart solar dryers have shown that controlled auxiliary heating can improve temperature management and drying performance (Mishra, Hauchhum, and Gupta 2022; Ibrahim et al. 2023). Reviews also identify auxiliary-energy integration, adaptability and reliable performance assessment as important directions in solar-drying research (Jha and Tripathy 2021; Kong et al. 2024; Rahman et al. 2025).

An important distinction remains between adding an electrical heater and engineering an electrical heating subsystem as a controllable process actuator. A resistive DC heater can respond rapidly to switching commands, making it suitable for compensating short-term thermal deficits in a dryer. Direct PV-to-DC heating also avoids the unnecessary PV-to-AC-to-DC conversion sequence that would arise if a conventional inverter were

License: This is an open access article under the CC BY 4.0 license: https://creativecommons.org/licenses/by/4.0/

used to supply a DC resistive element. However, PV voltage varies with irradiance, temperature and loading, so a regulated DC–DC interface is required if the heater is to operate close to its rated condition. The control system must then translate chamber-temperature error into a suitable switching command without introducing excessive thermal oscillation.

The present work isolates and evaluates this electrical/electronic function within a modular hybrid dryer. The wider dryer incorporates a solar air collector and a detachable charcoal biomass module, but the present paper focuses on the PV-powered DC heating path and its closed-loop temperaturecontrol function. The electrical architecture consists of two 350 W PV modules connected in parallel, an adjustable 800 W DC–DC converter, a 600 W, 35 V heater and an electronic feedback controller. The controller uses thermistor feedback, an SG3524 PWM stage, a C1815 driver and an IRFP4468 MOSFET to regulate the heater contribution.

This study is therefore concerned with five linked performance questions: whether the converter can maintain the required heater voltage under changing PV-side voltage; whether the heater can deliver its rated power with low variation; whether the feedback system can bring the chamber rapidly to a selected set-point; whether the chamber can remain stable after warm-up; and whether the resulting thermal condition supports effective moisture removal from plantain. The contribution is an experimental integration of PV power conversion, DC heating and closed-loop thermal control rather than a claim that PV heating or hybrid drying is itself a new principle.

2. MATERIALS AND METHOD

2.1 System Architecture

The fabricated dryer as presented in figure 1 was conceived as a modular electro-thermal system in which the principal heat sources could operate independently or in combination. Solar radiation was converted to sensible heat in the solar air collector; PV electricity was converted to controlled electrical heat through the DC–DC interface; and the detachable biomass unit supplied supplementary heat when solar input was inadequate. A continuously operating 12 V DC fan provided forced convection and supported moisture removal.

The present paper concentrates on the Photovoltaic Electric branch of the dryer. The PV array feeds the high-power DC path through protection and voltage regulation. The regulated 35 V output drives the 600 W resistive heater through the MOSFET switching stage. In parallel, a lowpower branch supplies the control electronics and fan. This separation prevents the high-power heater from becoming the dominant battery load and permits direct use of PV energy for heating.

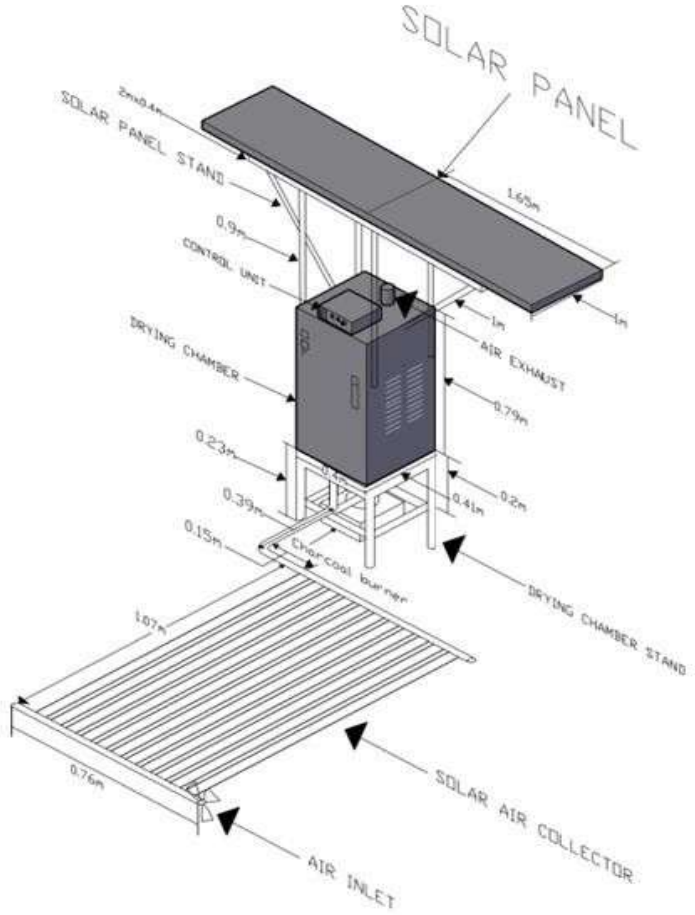


Figure 1: Isometric representation of the Hybrid dryer and major energy modules.

The physical prototype used an insulated drying chamber with five vertically arranged trays. The chamber was approximately 0.79 m high and 0.41 m × 0.41 m in plan. The solar air collector had an estimated area of approximately 2.0 m² and consisted of twelve absorber pipes, each approximately 1.092 m long with 50.8 mm internal diameter. The detachable charcoal burner was positioned beneath the chamber. The design airflow rate was 0.02 $m^3 s^{-1}$, corresponding to an air mass flow rate of approximately 0.024 kg s^{-1} at an assumed air density of 1.2 kg m^{-3}.

License: This is an open access article under the CC BY 4.0 license: https://creativecommons.org/licenses/by/4.0/

Corresponding Author: DARE, Aderonke Adekemi

2.2 PV Power and DC Heating Subsystem

Table 1. Principal electrical and control components of the evaluated subsystem.

Subsystem	Parameter	Design / rated value	Function
PV array	Modules	2 × 350 W, parallel	Primary electrical energy source
PV module	Vmp / Voc	33.7 V / 38.5 V	Nominal operating voltage
DC–DC converter	Rating	800 W; 24–40 V input; 35 V output	PV voltage regulation
Heater	Rating	600 W, 35 V DC; ≈17.14 A	Controlled auxiliary heat
Control	PWM controller	SG3524	Temperature-based duty control
Switching	Power device	IRFP4468 MOSFET	High-current heater switching
Driver	Transistor	C1815	Intermediate gate-drive stage
Fan	Rating	12 V, 0.5 A, 6 W	Continuous forced convection
Auxiliary supply	Battery	12 V, low-power loads	Fan and control circuits

The two PV modules were connected in parallel to retain approximately the module operating voltage while increasing the available current. The nominal array capacity was approximately 700 W. The 600 W heater required approximately 17.14 A at 35 V. Because the PV operating voltage was not fixed, an adjustable 800 W converter was selected with a 24-40 V input range and regulated 35 V output. The converter therefore provided approximately 25% power margin above the heater rating.

The auxiliary battery was not used as the principal source for the 600 W heater. It was assigned to the fan and control circuits. This design choice reduced the required storage capacity and maintained the high-power heating path as a direct PV-to-DC energy route. The electrical arrangement consequently combined renewable generation, power electronics and thermal actuation without an inverter, table 1 thus gives detailed description of some of the components used.

2.3 Closed Loop Temperature Control

Temperature regulation was implemented as a feedback loop as illustrated in figure 2. A thermistor installed in the chamber produced a temperature-dependent electrical signal. The sensing signal was conditioned and combined with the selected temperature input before being applied to the SG3524 PWM controller. The SG3524 generated the switching control signal; the C1815 transistor provided an intermediate driver stage; and the IRFP4468 N-channel MOSFET modulated the highpower heater.

The operating principle was straightforward. When chamber temperature was below the selected set-point, the controller increased the effective electrical heating contribution. As the temperature approached the set-point, the control action reduced the heater contribution. The fan remained in continuous operation so that the heat supplied by the heater and other heat sources was distributed through the chamber and moisture-laden air was removed.

The experimental set-point was 60 °C. The evaluation therefore treated temperature tracking and steady-state variability as explicit engineering metrics rather than using temperature only as a descriptive operating condition.

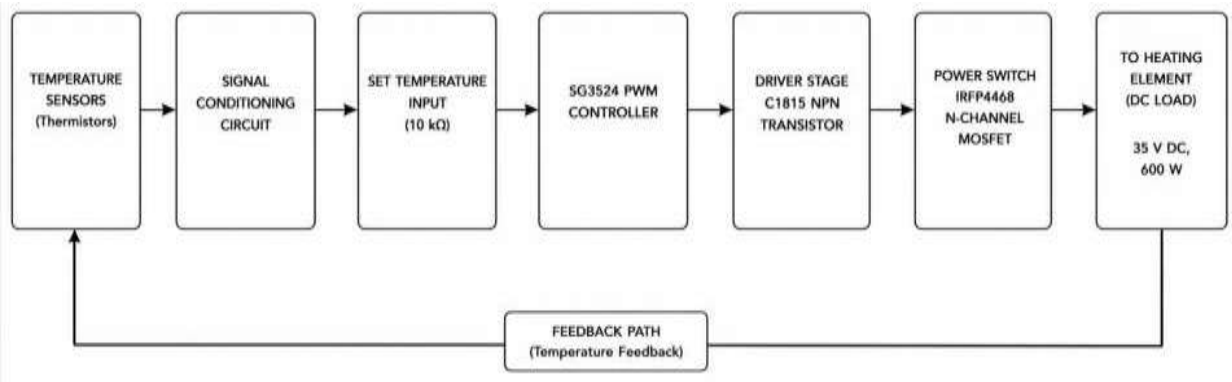


Figure 2. Closed-loop electronic temperature-control pathway.

2.4 Thermal and Experimental Conditions

Table 2. Experimental conditions and principal test parameters.

Parameter	Value	Purpose
Batch load	10 kg fresh plantain	Representative experimental load
Initial moisture content	65% wet basis	Starting drying condition
Target moisture content	≈10% wet basis	Experimental endpoint
Control set-point	60 °C	Controlled chamber condition
Airflow rate	0.02 $m^3 s^{-1}$	Forced convection
Chamber	0.79 m × 0.41 m × 0.41 m	Drying enclosure

License: This is an open access article under the CC BY 4.0 license: https://creativecommons.org/licenses/by/4.0/

Tray arrangement	5 vertical trays	Product distribution
Electrical/control sampling	15 min	Performance measurements
Electrical test duration	5 h	Converter/heater/control evaluation
Drying test duration	8 h	Moisture-removal evaluation

Unripe plantain was used as the representative crop. A 10 kg batch was distributed across five trays with approximately uniform slice thickness and minimal overlap. Chamber temperature, heater voltage and current, converter input and output voltage and current, and product mass were recorded at 15-min intervals. The electrical control test was analysed over five hours, while the drying trajectory was followed for eight hours, table 2 shows the experimental conditions and major test parameters.

The thermal design of the complete dryer required more heat than the electrical heater alone could provide; the 600 W element was therefore treated as a controllable auxiliary heat source. This distinction is important because the objective of the PV branch was not to supply the complete drying load but to provide responsive electrical heat when the chamber temperature tended to fall below the selected set-point.

2.5 Performance Metrics

The performance of the PV-powered DC heating subsystem was evaluated using electrical conversion efficiency, heater power, temperature-tracking error, drying rate and coefficient of variation as expressed in table 3. These metrics were selected to assess the efficiency of transferring electrical power from the PV array to the heater, the stability of heater output, the accuracy of chamber-temperature regulation relative to the 60 °C set-point, and the resulting drying response. Converter efficiency was calculated from the ratio of output to input electrical power, while heater power was determined from measured voltage and current. Temperaturetracking accuracy was assessed using the mean absolute temperature error (MATE), and drying rate was calculated from the change in product mass over a specified time interval. The coefficient of variation (CV) was used to quantify relative variability in measured performance. Together, these equations provide a quantitative basis for evaluating the electrical and thermal response of the system and relating its control performance to the observed plantain-drying process.

Table 3. Performance equations used for experimental evaluation.

Metric	Expression	Interpretation
Converter efficiency	$\eta_{conv} = (P_{out} / P_{in}) \times 100$	Pout = Vout Iout; Pin = Vin Iin
Heater power	$P_h = V_h I_h$	V_h and I_h are measured heater voltage and current
Absolute temperature error	$Ei = \lvert Ti - Tset \rvert$	T_{set} = 60 °C, T_i is the measured chamber temperature at observation i
Mean absolute temperature error	$MATE = (1/n)\ \Sigma\lvert Ti - Tset \rvert$	Tracking accuracy
Drying rate	$DR = (M_{t1} - M_{t2})/(t_2 - t_1)$	M_{t1} and M_{t2} are plantain masses and time t_1 and t_2
Coefficient of variation	CV = (SD / mean) × 100	Relative variability

3. RESULTS

3.1 Chamber Temperature Response

The chamber exhibited a rapid warm-up followed by a stable operating period. As shown in figure 4, Temperature increased from 30.4 °C at the start of the test to 40.9 °C at 0.25 h, 50.8 °C at 0.50 h, 58.7 °C at 0.75 h and 59.7 °C at 1.00 h. After approximately one hour, the measured temperature remained close to the 60 °C set-point, with the reported steady-state range approximately 60.0–
60.3 °C. The quantitative results presented in table 4 further confirm this stability, showing a steady-state mean was 60.13 °C, with a standard deviation of 0.11 °C and coefficient of variation of 0.18%. These results indicate that the heater, converter and feedback controller operated as a coordinated system rather than producing large heating oscillations by maintaining the chamber temperature.

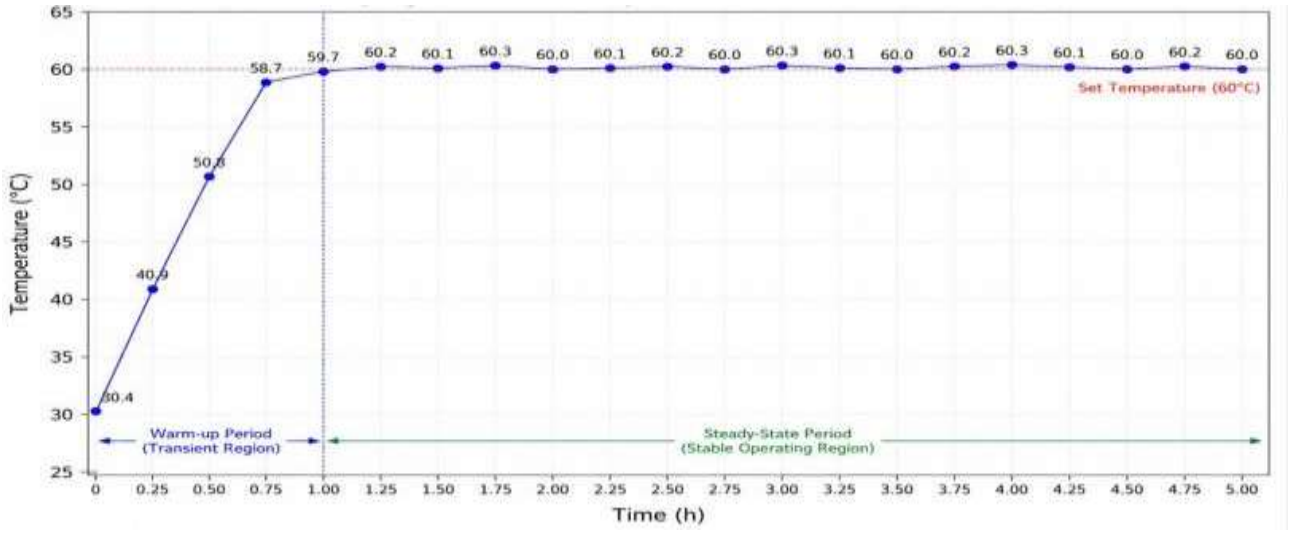


Figure 4: Chamber temperature response during the electrical and control test.

License: This is an open access article under the CC BY 4.0 license: https://creativecommons.org/licenses/by/4.0/

Table 4: Chamber-temperature stability results

Indicator	Result
Set-point	60 °C
Initial chamber temperature	30.4 °C
Temperature at 1 h	59.7 °C
Steady-state mean	60.13 °C
Standard deviation	0.11 °C
Coefficient of variation	0.18%
Approximate steady-state range	60.0–60.3 °C

3.2 Heater Power Stability

During the warm-up period, heater power increased toward the rated operating level. As shown in figure 5, the heater subsequently maintained a stable power output during steady-state operation, with the measured power ranging from 596.70 to 603.68 W. The mean heater power was 600.13 W, with a standard deviation of 1.97 W and a coefficient of variation of 0.33%. These results demonstrate that the DC–DC converter and electronic switching stage delivered power close to the heater's rated 600 W, with minimal variation. This stability is important for the closed-loop temperature-control system because consistent heater power supports the maintenance of the desired chamber temperature during drying.

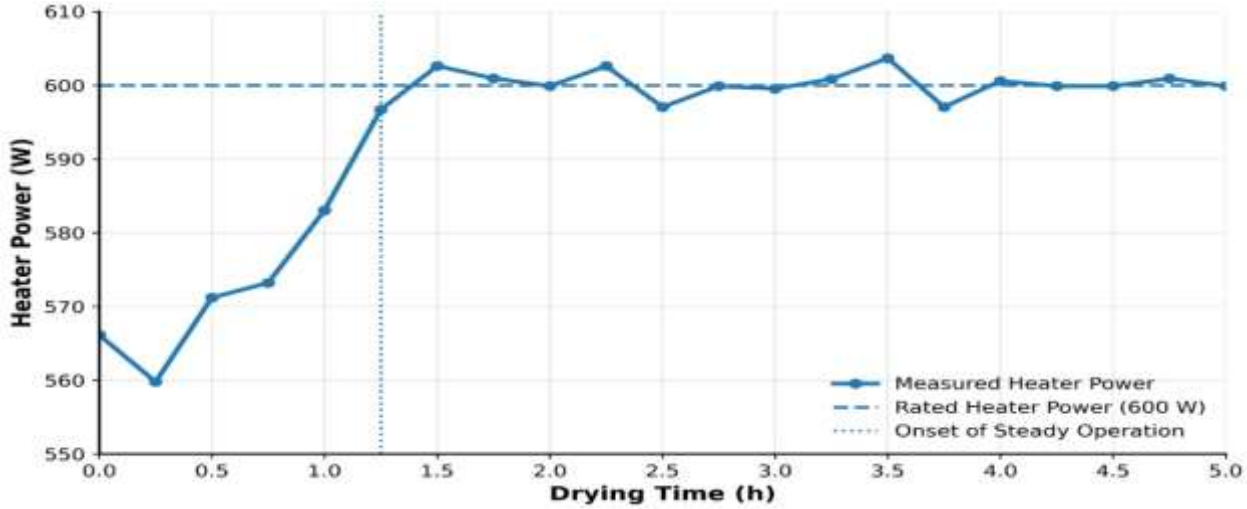


Figure 5: Heater power response during the electrical and control test.

3.3 Temperature Tracking Accuracy

The temperature-tracking response demonstrates the accuracy of the closed-loop control system in maintaining the chamber temperature near the 60 °C set-point. As illustrated in Figure 6, the absolute temperature error decreased from 29.6 °C at the beginning of the test to 19.1 °C at 0.25 h, 9.2 °C at 0.50 h, 1.3 °C at 0.75 h and 0.3 °C at 1.00 h. From approximately 1.25 h onward, the error remained within 0.0-0.3 °C. The performance indicators summarized in Table 5 show a mean absolute temperature error (MATE) of 0.13 °C and a maximum absolute error of 0.30 °C. These results indicate that the electronic feedback controller achieved close temperature tracking after the initial warm-up period, supporting stable thermal conditions for the plantain drying process.

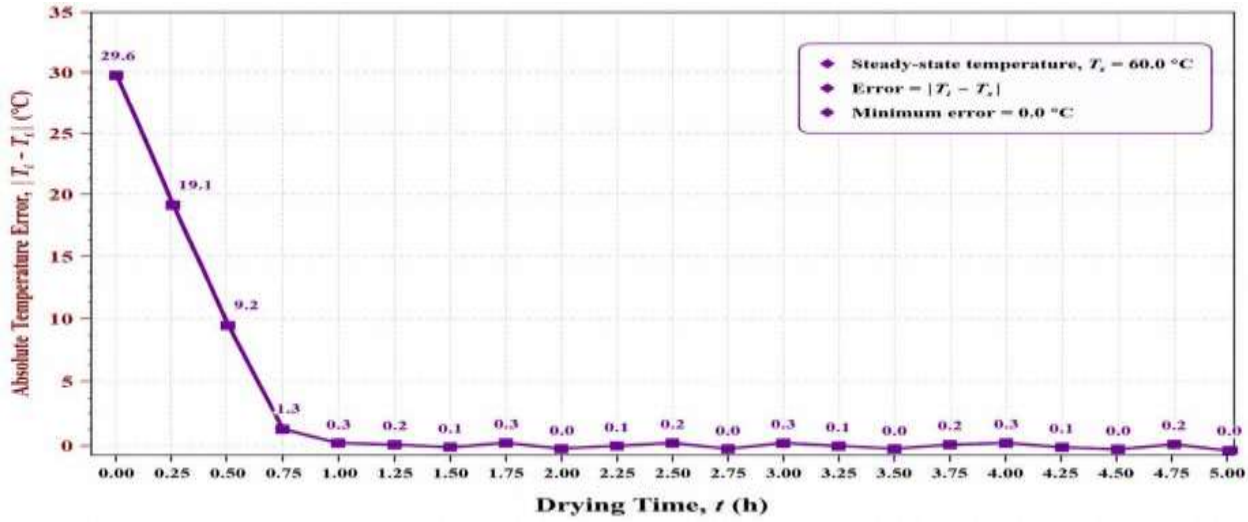


Figure 6: Absolute chamber-temperature tracking error relative to the 60 °C set-point.

License: This is an open access article under the CC BY 4.0 license: https://creativecommons.org/licenses/by/4.0/

Table 5: Temperature-tracking performance.

Tracking indicator	Result
Mean absolute temperature error	0.13 °C
Maximum absolute error	0.30 °C
Steady-state error range	0.0–0.3 °C
Time to approximately 59.7 °C	1.0 h

3.4 DC-DC Converter Performance

The performance of the DC–DC converter was evaluated in terms of voltage regulation, power transfer and conversion efficiency. Figure 7 shows that the converter maintained an output voltage of 34.70–35.00 V despite variations in the PV input voltage from 28.50 to 33.71 V. As presented in Figure 8, the input power varied around the mid-650 W level, while the output power remained close to the 600 W required by the heating element. Figure 9 further illustrates the converter's efficiency response, which ranged from 90.70% to 91.70%. The summary in Table 6 confirms a mean conversion efficiency of 91.30%, a standard deviation of 0.29% and a coefficient of variation of 0.32%. These results demonstrate that the converter provided effective voltage regulation and relatively consistent power conversion under the tested operating conditions. Maintaining a nearconstant output voltage and stable power delivery is essential for supplying the DC heater reliably and supporting the closed-loop control system in maintaining the desired drying-chamber temperature.

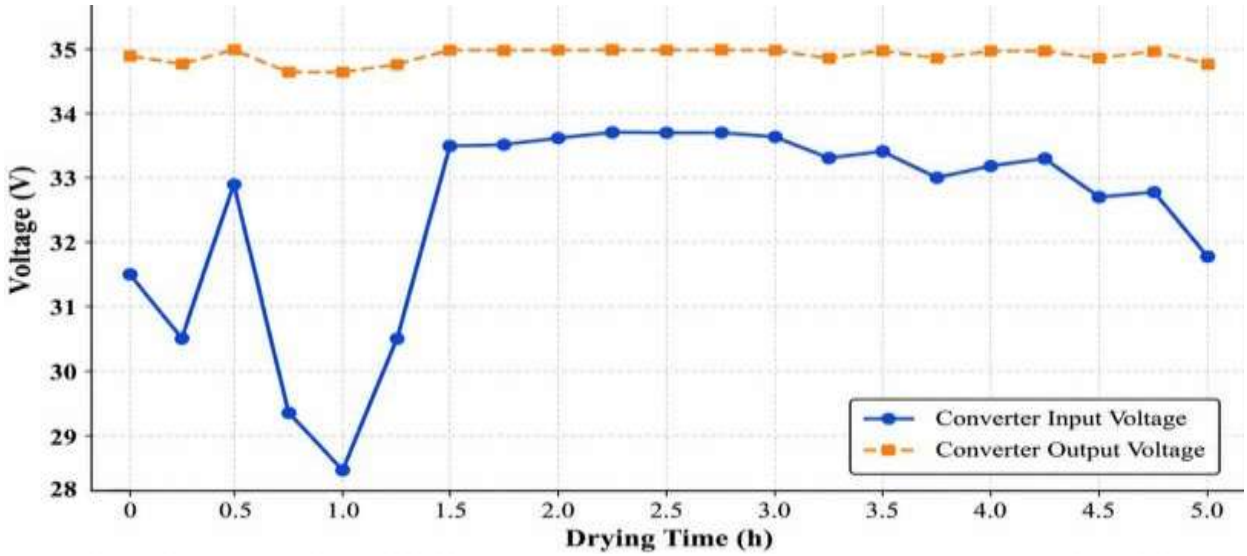


Figure 7: Converter input and output voltage during the test.

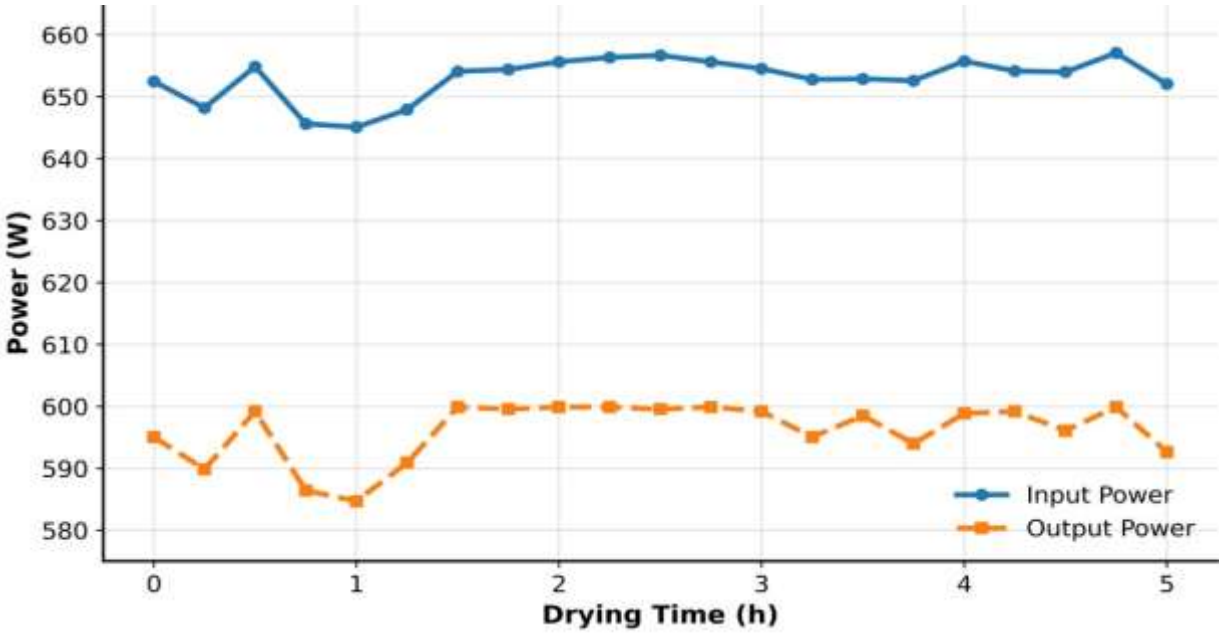


Figure 8: Converter input and output power during the test.

License: This is an open access article under the CC BY 4.0 license: https://creativecommons.org/licenses/by/4.0/

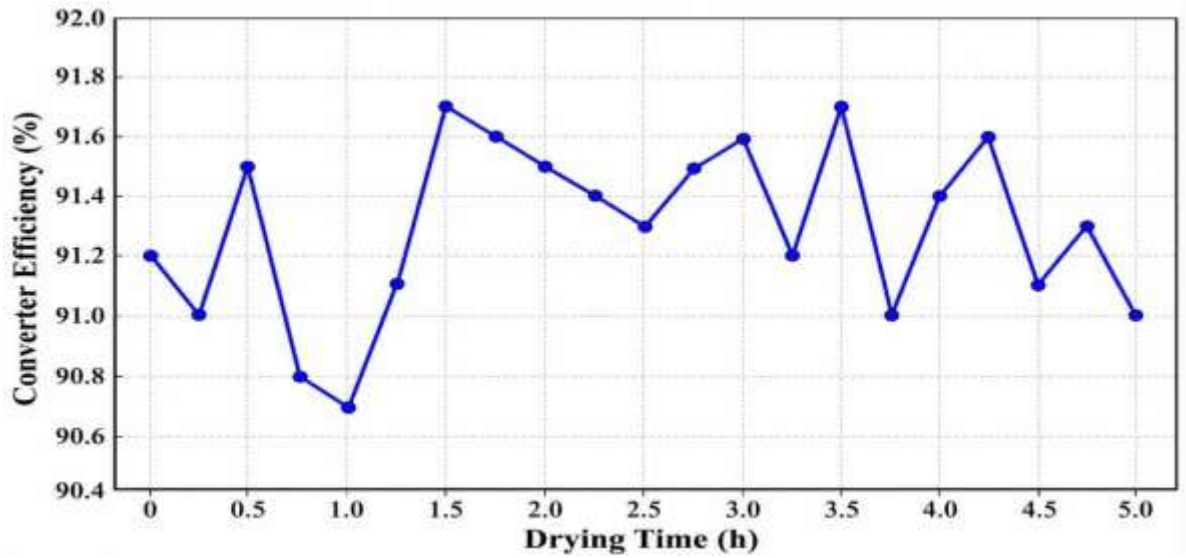


Figure 9: Converter efficiency during the test.

Table 6: DC–DC converter performance summary.

Converter metric	Result
Input-voltage range	28.50–33.71 V
Output-voltage range	34.70–35.00 V
Efficiency range	90.70–91.70%
Mean efficiency	91.30%
Standard deviation	0.29%
Coefficient of variation	0.32%

3.5 Plantain Drying Response

The plantain-drying response was evaluated by monitoring chamber temperature, product mass, moisture content and drying rate over the eight-hour experiment. As shown in Figure 10, the drying rate increased during the initial heating period, reaching a maximum of approximately 1.29 kg h^{-1} at 1.75 h, when the chamber temperature was 60.3 °C. Thereafter, the drying rate declined progressively while the chamber temperature remained close to the 60 °C set-point, indicating that the reduction in drying rate was associated increasingly with internal moisture migration rather than temperature instability. The selected measurements presented in Table 7 further show that the plantain mass decreased from 10.00 kg to 3.89 kg, while the moisture content reduced from 65% to approximately 10% (wet basis) within eight hours. The drying rate fell to approximately 0.04 kg h^{-1} at the end of the test. These results demonstrate that the PV-powered heating system and closed-loop temperature controller maintained the required drying temperature while supporting progressive moisture removal from the plantain.

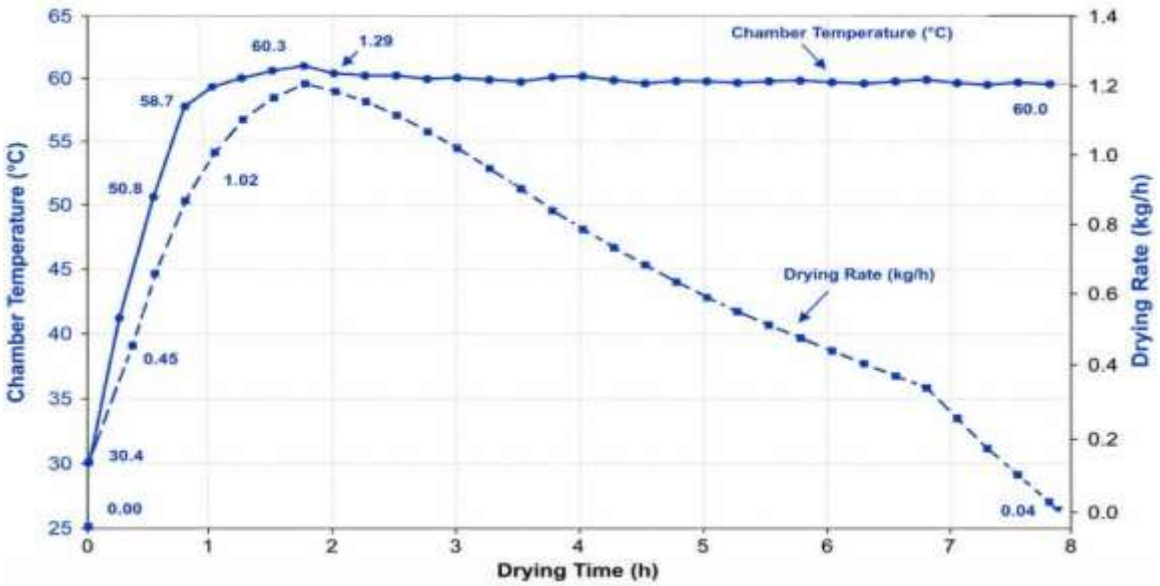


Figure 10: Combined chamber temperature and drying-rate response during the 8-h plantain drying test

License: This is an open access article under the CC BY 4.0 license: https://creativecommons.org/licenses/by/4.0/

Corresponding Author: DARE, Aderonke Adekemi

Table 7: Selected measurements from the plantain drying experiment

Time (h)	Temp. (°C)	Mass (kg)	Moisture (%)	Drying rate (kg h^{-1})
0.00	30.40	10.00	65.00	—
0.50	50.80	9.71	63.95	0.76
1.00	59.70	9.18	63.86	1.14
1.50	60.10	8.55	59.07	1.27
1.75	60.30	8.23	57.47	1.29
2.50	60.20	7.30	51.99	1.21
4.00	60.30	5.77	39.38	0.88
5.00	60.00	5.02	30.25	0.69
6.00	60.30	4.44	21.09	0.53
7.00	60.10	4.01	12.80	0.31
8.00	60.00	3.89	10.00	0.04

4. DISCUSSION

4.1 Significance of Closed Loop Control

The central engineering result is the observable chain from variable PV input to controlled chamber temperature. PV-side voltage changed substantially during the test, but the converter maintained an output close to 35 V. The heater consequently operated near its rated 600 W level, while the temperature feedback loop adjusted the switching action to maintain the chamber near the setpoint. The system therefore demonstrates that the electrical subsystem was not merely a source of energy; it was an active thermal-process actuator. The mean converter efficiency of 91.30% indicates that most of the PV-side electrical input was transferred to the heater, while the low coefficient of variation indicates consistent conversion performance over the test interval. Stable conversion is particularly important in direct PV heating because power-stage disturbances can become temperature disturbances if the heater output is not regulated.

The temperature results demonstrate the practical advantage of closed-loop electronic regulation over uncontrolled auxiliary heating. The chamber reached approximately 59.7 °C in one hour and then remained within about ±0.3 °C of the 60 °C target. The MATE of 0.13 °C indicates close setpoint tracking, while the 0.18% coefficient of variation indicates very low steady-state dispersion. These results are consistent with the broader direction of smart hybrid drying, in which auxiliary heating and electronic control are used to improve operation under variable weather conditions. Ibrahim et al. (2023), for example, demonstrated a hybrid smart solar dryer with controlled auxiliary heating for herb drying. The present study differs in emphasis by experimentally quantifying the PV-side voltage regulation, DC heating power stability and feedback accuracy of the electrical subsystem. The novelty is therefore the integration and measured electrical-control performance and not the general concept of hybrid drying.

4.2 Comparison with Selected Studies

Earlier hybrid drying studies establish the feasibility of combining solar energy with auxiliary heat sources, while recent smart-dryer research demonstrates the value of automatic temperature regulation (Kiburi et al. 2020; Mishra, Hauchhum, and Gupta 2022; Ibrahim et al. 2023). The present work extends this engineering direction by treating the PV-electric path as a measurable subsystem. In particular, the converter output, heater power, temperature tracking and process response are evaluated as a connected chain. The modular arrangement also provides operational flexibility. The solar air collector can supply the principal sensible heat during favourable solar conditions; the PV heater can provide responsive trimming heat; and the detachable biomass module can support operation when solar availability is inadequate. This configuration avoids dependence on a large battery for the 600 W heater and permits individual modules to be maintained or replaced without redesigning the complete dryer.

4.3 Practical Implications and Limitations

The results support the technical feasibility of direct PV-powered DC heating as an auxiliary heat source for agricultural drying when coupled with regulated power conversion and feedback control. The configuration eliminates the need for an inverter in the heating path and therefore reduces the number of major conversion stages between the PV array and resistive heater. It also provides a responsive thermal actuator that can be modulated according to chamber-temperature error.

The evaluation represents a controlled prototype test rather than a complete seasonal or commercial validation. The available measurements do not provide a complete experimental energy-contribution breakdown among the solar-thermal, PV-electric and biomass pathways for every operating mode; therefore, a universal whole-dryer efficiency is not claimed. Product-quality attributes such as colour, texture, nutrient retention and microbial stability were also outside the scope of the present study.

4.5 Engineering Significance

The principal contribution of the work is the integration of renewable-energy conversion and electronic process control in an agricultural dryer. The PV array provides renewable electrical energy; the converter produces a controlled DC supply; the resistive heater converts that energy directly to heat; and the feedback controller regulates the resulting process temperature. This architecture makes the electrical/electronic contribution explicit in a field that is often evaluated mainly through thermal efficiency or final moisture content.

The measured results support this interpretation. A mean converter efficiency of 91.30% was accompanied by only 0.32% coefficient of variation; the heater delivered 600.13 W with 0.33% coefficient of variation; and the chamber maintained 60.13 °C with a 0.13 °C mean absolute tracking error. The agreement of these indicators shows that stable electrical delivery translated into stable thermal operation.

The plantain drying response further demonstrates process relevance. The maximum drying rate occurred during the early period when thermal driving force was being established. Once the chamber had stabilized, the rate decreased progressively as easily removable moisture was depleted. The electrical system therefore achieved its principal role: maintaining the selected thermal condition while the product drying kinetics evolved independently.

License: This is an open access article under the CC BY 4.0 license: https://creativecommons.org/licenses/by/4.0/

Corresponding Author: DARE, Aderonke Adekemi

5. CONCLUSION

An experimentally evaluated PV-powered DC heating subsystem with closed-loop temperature control was successfully integrated into a modular hybrid agricultural dryer. The system used two 350 W PV modules in parallel, an 800 W adjustable DC–DC converter, a 600 W/35 V resistive heater and thermistor-based feedback through an SG3524 PWM controller, C1815 driver and IRFP4468 MOSFET.

The converter regulated a variable PV input of 28.50–33.71 V to 34.70–35.00 V at the heater, with a mean efficiency of 91.30% and coefficient of variation of 0.32%. The heater delivered a mean steady-state power of 600.13 W with a coefficient of variation of 0.33%. Chamber temperature reached 59.7 °C within approximately one hour and stabilized at 60.13 °C, with 0.11 °C standard deviation, 0.18% coefficient of variation, 0.13 °C mean absolute temperature error and 0.30 °C maximum deviation.

During the associated 8-h plantain test, a 10 kg load at 65% wet-basis moisture content was reduced to approximately 10%, while the drying rate peaked at 1.29 kg h^{-1} and declined to 0.04 kg h^{-1} as the process entered the falling-rate period. The results indicate that direct PV to DC heating combined with regulated power conversion and closed-loop control is technically suitable as a responsive auxiliary heat source for modular hybrid dryers.

Future work should quantify solar irradiance, collector inlet/outlet temperatures, airflow, biomass consumption and integrated electrical energy simultaneously so that complete energy balances can be established for solar-only, PV-assisted, biomass-assisted and combined modes. Repeated tests under different weather and loading conditions, together with product-quality assessment and electrical safety/thermal-management validation, are also required before scale-up.

REFERENCES

1) Akinyemi, O. F., A. A. Adebayo, and S. A. Oladipo. 2022. “Assessment of Post-harvest Losses of Plantain (Musa paradisiaca) in Selected Markets in South-Western Nigeria.” Journal of Agricultural Extension 26 (1): 56–65. https://doi.org/10.4314/jae.v26i1.7.
2) Amer, B. M. A., M. A. Hossain, and K. Gottschalk. 2010. “Design and Performance Evaluation of a New Hybrid Solar Dryer for Banana.” Energy Conversion and Management 51 (4): 813– 820. https://doi.org/10.1016/j.enconman.2009.11.016.
3) Baddadi, Sara, Safa Skouri, Rabeb Ayed, Laxmikant Jathar, and Salwa Bouadila. 2023. “Performance Investigation of an Innovative Solar Heating Unit for a Powered Self-Sustained Solar Dryer.” Applied Thermal Engineering 233: 121173. https://doi.org/10.1016/j.applthermaleng.2023.121173.
4) Bhange, Saurabh S., and Sanjay S. Deshmukh. 2025. “Design and Testing of a Solar Biomass Hybrid Dryer for Vegetables Drying.” International Journal of Mechanical Engineering 12 (11): 110–120. https://doi.org/10.14445/23488360/IJME-V12I11P110.
5) Duque-Dussán, Eduardo, Juan R. Sanz-Uribe, and Jan Banout. 2023. “Design and Evaluation of a Hybrid Solar Dryer for Postharvesting Processing of Parchment Coffee.” Renewable Energy 215: 118961. https://doi.org/10.1016/j.renene.2023.118961.
6) Elangovan, Elavarasan, and Sendhil Kumar Natarajan. 2022. “Experimental Research of Drying Characteristic of Red Banana in a Single Slope Direct Solar Dryer Based on Natural and Forced Convection.” Food Technology and Biotechnology 59 (2): 215–225. https://doi.org/10.17113/ftb.59.02.21.6876.
7) El-Sebaii, A. A., and S. M. Shalaby. 2012. “Solar Drying of Agricultural Products: A Review.” Renewable and Sustainable Energy Reviews 16 (1): 37–43. https://doi.org/10.1016/j.rser.2011.07.134.
8) Ibrahim, Ayman, Islam Elsebaee, Alia Amer, Galal Aboelasaad, Abdelalim El-Bediwy, and Mohamed El-Kholy. 2023. “Development and Evaluation of a Hybrid Smart Solar Dryer.” Journal of Food Science 88 (9): 3859–3878. https://doi.org/10.1111/1750-3841.16713.
9) Jha, Aprajeeta, and P. Tripathy. 2021. “Recent Advancements in Design, Application, and Simulation Studies of Hybrid Solar Drying Technology.” Food Engineering Reviews 13 (2): 375–410. https://doi.org/10.1007/s12393-020-09223-2.
10) Kiburi, F. G., C. L. Kanali, G. M. Kituu, P. O. Ajwang, and E. K. Ronoh. 2020. “Performance Evaluation and Economic Feasibility of a Solar-Biomass Hybrid Greenhouse Dryer for Drying Banana Slices.” Renewable Energy Focus 34: 60–68. https://doi.org/10.1016/j.ref.2020.06.009.
11) Koli, Chandra Shekhar, M. K. Gaur, and Pushpendra Singh. 2022. “Energy and Exergy Assessment of a Novel Parabolic Hybrid Active Greenhouse Solar Dryer.” Solar Energy 245: 228–242. https://doi.org/10.1016/j.solener.2022.09.021.
12) Kong, Decheng, Yunfeng Wang, Ming Li, and Jingkang Liang. 2024. “A Comprehensive Review of Hybrid Solar Dryers Integrated with Auxiliary Energy and Units for Agricultural Products.” Energy 293: 130640. https://doi.org/10.1016/j.energy.2024.130640.
13) Mahajan, K. M., V. H. Patil, and T. A. Koli. 2024. “Design Analysis of an Innovative Solar Biomass Hybrid Dryer for Drying Turmeric.” Hyperfine Interactions 245: 32. https://doi.org/10.1007/s10751-024-01965-3.
14) Mawire, Ashmore, Masodi Ramokali, Molebogeng Mothupi, and Maarten Vierschot. 2024. “An Experimental Evaluation of Drying Banana Slices Using a Novel Indirect Solar Dryer Under Variable Conditions.” Heliyon 10 (5): e28268. https://doi.org/10.1016/j.heliyon.2024.e28268.
15) Mishra, Laxman, Lalhmingsanga Hauchhum, and Rajat Gupta. 2022. “Development and Performance Investigation of a Novel Solar-Biomass Hybrid Dryer.” Applied Thermal Engineering 211: 118492. https://doi.org/10.1016/j.applthermaleng.2022.118492.
16) Rahman, M. A., S. M. M. Hasnain, P. Paramasivam, R. Zairov, and A. G. Ayanie. 2025. “Solar Drying for Domestic and Industrial Applications: A Comprehensive Review of Innovations and Efficiency Enhancements.” Global Challenges 9 (3): 2400301. https://doi.org/10.1002/gch2.202400301.
17) Rawat, Pratish, and Sourav Kumar. 2022. “Designing and Construction of Low Cost Hybrid Photovoltaic-Thermal (PVT) Solar Dryer.” International Journal of Creative Research Thoughts 10 (5): 231–238.

License: This is an open access article under the CC BY 4.0 license: https://creativecommons.org/licenses/by/4.0/

Corresponding Author: DARE, Aderonke Adekemi